

Attitude control in spacecraft orbit-raising using a reduced quaternion model

Yaguang Yang*

*Division of Engineering, Office of Research, US Nuclear Regulatory Commission,
21 Church Street, Rockville, MD 20850, USA*

(Received January 18, 2014, Revised May 13, 2014, Accepted May 20, 2014)

Abstract. Orbit-raising is an important step to place spacecraft from parking orbits into working orbits. Attitude control system design is crucial in the success of orbit-raising. Several text books have discussed this design and focused mainly on the traditional methods based on single-input single-output (SISO) transfer function models. These models are not good representations for many orbit-raising control systems which have multiple thrusters and each thruster has impact on the attitude defined by all outputs. Only one published article is known to use a more suitable multi-input multi-output (MIMO) Euler angle model in spacecraft orbit-raising attitude control system design. In this paper, a quaternion based MIMO model for the orbit-raising attitude control system design is proposed. The advantages of using quaternion based model for orbit-raising control system designs are (a) there is no need for mathematical transformations because the attitude measurements are normally given by quaternion, (b) quaternion based model does not depend on rotational sequences, which reduces the chance of human errors, and (c) the singular point of reduced quaternion model is the farthest from the operational point where linearization is performed. We will show that performance of quaternion model based design will be as good as the performance of Euler angle model based design for orbit-raising problem.

Keywords: reduced quaternion model; spacecraft; orbit-raising; attitude control; pulse width modulation

1. Introduction

Multiple modes of spacecraft attitude control systems are desired because a spacecraft needs to perform different tasks to achieve its missions during the spacecraft life cycle, such as attitude maneuver, attitude control in normal operational mode, and attitude control in orbit-raising mode. Euler angle models and quaternion models are most popular models for spacecraft control system designs. Attitude maneuver controls using either quaternion or Euler angle models have been extensively discussed in several textbooks, such as Sidi (1997), Wie (1998), Wertz (1978). Attitude control system designs in normal operational mode using various models, such as Euler angle models and quaternion models, single-input transfer function models and multi-input state space models, have been the main topics in spacecraft control system designs and have been investigated in many research papers and textbooks, for example, Sidi (1997), Wie (1998), Wertz

*Corresponding author, Ph.D., E-mail: yaguang.yang@verizon.net

(1978), Wie *et al.* (1989), Boskovic *et al.* (2001), Wallsgrove and Akella (2005), Wen and Kreutz-Delgado (1991), Paielli and Bach (1993), Won (1999). Most discussions on orbit-raising attitude control are based on SISO transfer function models Sidi (1997), Wie (1998) and the designs use single loop compensation. Since orbit-raising using single-input model design is difficult to stabilize the MIMO spacecraft system, NASA suggested using spin stabilized thrust control (Noll *et al.* 1971). This design strategy needs some additional fuel consumption to spin the spacecraft during the thrust and de-spin the spacecraft after the thrust. As multiple thrusters are used during orbit-raising and the effect of each thruster has impact on all outputs (roll, pitch, and yaw), a good design model should be an MIMO state space model and the ideal design method should consider multi-input multi-output features of the system. Very few designs on orbit-raising using MIMO models have been reported. One noticeable work is by Stoltz *et al.* (1998) which described the OrbView-2 spacecraft orbit-raising control system design using an Euler angle model. The real flight experience reported by Stoltz *et al.* (1998) shows that this design is very successful and does not need to spin the spacecraft during the thrust because a more advanced control method can do a better work than traditional methods.

In a series of recent papers, Yang (2010, 2012, 2014) proposed to adopt a reduced quaternion model in spacecraft attitude control system design. For the operational mode, the LQR design for attitude control system based on a reduced quaternion model has an analytic solution which is directly related to the desired closed-loop pole locations. The designed linear feedback controller globally stabilizes the original nonlinear spacecraft system (Yang 2012). Moreover, the analytic LQR design is a robust pole assignment design which is insensitive to the modeling error and is proved to have a good performance of disturbance rejection (Yang 2014).

In this paper, we extend the method developed in Yang (2010, 2012) to the orbit-raising attitude control system design. Since the linearized reduced quaternion model for orbit-raising control system is fully controllable (Yang 2010), it is possible to directly apply many the modern linear system design methods to spacecraft attitude control system designs. We will show that similar to the Euler angle model based design, the quaternion based design can avoid spinning the spacecraft during the thrust and de-spinning the spacecraft after the thrust, which reduces fuel consumptions; and the performance of the new design is comparable to the performance of the design given by Stoltz *et al.* (1998). However, several other factors make the quaternion model-based design more attractive. First, quaternion is most likely used in attitude determination systems (Yang 2012a), therefore, there is no need of using mathematical transformation from quaternion to Euler angles. Second, the quaternion model does not depend on rotational sequence, which reduces the chance of human errors in the design process. Finally, the linearized quaternion model has a singular point that is the farthest to the operational point where the linearization is performed, while Euler angle model has a nondeterministic singular point depending on the rotational sequence.

Since flight test is very expensive, most new spacecraft attitude estimation and control design methods are first tested in some simulation environment, for example, Chan *et al.* (2010), Sanyal *et al.* (2008), Kim *et al.* (2008), Chen *et al.* (2007), Bras *et al.* (2013), Martin and Salaun (2010). We will also demonstrate the design performance by a simulation test.

In the next section, a linearized reduced quaternion model for OrbView-2 orbit-raising system is derived (the same strategy can easily be applied to any orbit-raising thruster configuration). In Section 3, LQR design (Athans and Falb 1966) and pulse width modulation is discussed. In Section 4, this design is then used to calculate the feedback matrices for both the reduced quaternion model and the Euler angle model, that have the same parameters of OrbView-2

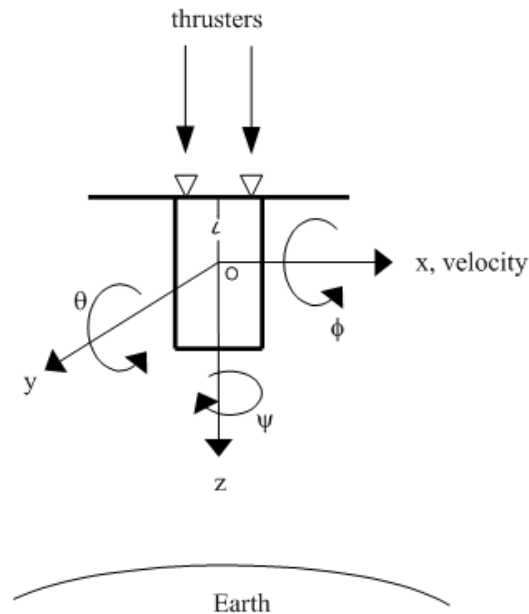


Fig. 1 Spacecraft coordinates definition in parking-orbit

spacecraft and the same design parameters proposed in (Stoltz *et al.* 1998). These two designs are applied to the original nonlinear spacecraft system models in the simulation. The responses of the closed-loop nonlinear system for these two different designs are compared. The conclusions are summarized in the last section.

2. Reduced quaternion model for orbit-raising

The quaternion model for orbit-raising depends on the spacecraft design. In this section, the OrbView-2 spacecraft (Stoltz *et al.* 1998) is used as an example to describe the modeling process. OrbView-2 has a momentum wheel with the angular momentum vector aligned parallel to the orbit-normal ($-y$ axis), the spacecraft attitude control in normal operation mode is performed by this wheel and 3 magnetic torque rods. The parking-orbit of OrbView-2 is about 300 km above the Earth surface, and the working-orbit is about 705 km above the Earth surface. The spacecraft desired attitude at parking-orbit, which coincides with the local vertical local horizontal (LVLH) frame, is shown as in Fig. 1. The origin of this attitude frame is defined at the center of mass of the spacecraft which is denoted as "o". Orbit-raising is performed by 4 fixed 1 (lbf) (lbf=4.448 Newton) thrusters with on/off switches which are mounted on the anti-nadir face of the spacecraft in each corner of a square with a side length of $2d$ as shown in Fig. 2. The thrusters point to $+z$ direction (into the page) and are canted 5° degree from z -axis (in the directions depicted by the arrows) to produce moments to maintain the spacecraft attitude during the burns. These thruster are mounted a distance l (m) along $-z$ axis from the spacecraft center of mass (and the coordinate system origin). The similar design is used in ROCSAT-3 spacecraft as reported in Show *et al.* (2003).

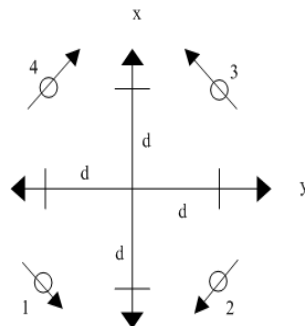


Fig. 2 Thruster mounting geometry

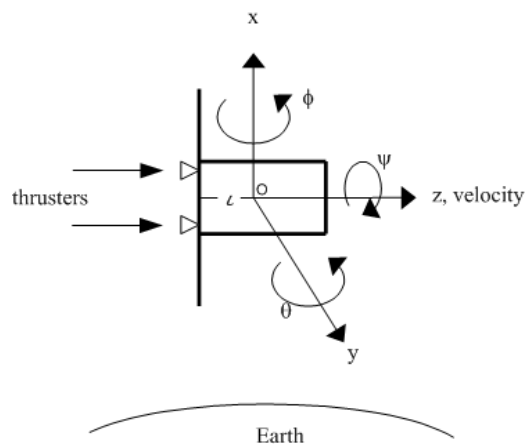


Fig. 3 Spacecraft coordinates definition in orbit-raising

The spacecraft thrust control system of OrbView-2 is designed to transfer the spacecraft from the parking orbit to a sun-synchronous orbit. The attitude of the spacecraft before orbit-raising is stabilized in the nadir-pointing orientation. To perform the task of orbit-raising, the spacecraft needs to rotate 90° degree around y-axis so that the thrusters, which are mounted on the anti-nadir face, are aligned parallel to the velocity vector. This is a typical situation that spacecraft attitude maneuver is required. The attitude maneuver is a simple operation and has been fully studied in textbooks, such as Sidi (1997) using simple control methods; and in some recently published papers, such as (Show *et al.* 2003), using more advanced control methods. This paper will not discuss the control of this attitude maneuver. Instead, it will focus on the orbit-raising attitude control system designs.

To conduct Hohmann transfers to raise the orbit (for more details on Hohmann transfer and orbit-raising operational requirements, the readers are referred to Sidi (1997) and Wie (1998)), OrbView-2 uses the momentum wheel to provide the torque to rotate the spacecraft $\pm 90^\circ$ degrees to align the thrusters along with or anti-parallel to the velocity vector (see Fig. 3). At this orientation, the thruster burns will raise the spacecraft orbit. Let h_w be the angular momentum produced by the momentum wheel. Let the rotation of the spacecraft body frame relative to the

frame described by Fig. 3 (with x -axis aligned with anti-nadir direction) represented in the body frame be given by the quaternion

$$\bar{q} = [q_0 \quad q_1 \quad q_2 \quad q_3]^T = [q_0 \quad q^T]^T = \left[\cos\left(\frac{\alpha}{2}\right) \quad \vec{e}^T \sin\left(\frac{\alpha}{2}\right) \right]^T$$

where \vec{e} is the rotational axis and α is the rotational angle ($\alpha=0$ when the spacecraft is perfectly aligned with the frame described by Fig. 3). Let $W=[w_x \ w_y \ w_z]^T$ be the angular rate of the rotation represented in the body frame

$$J = \begin{bmatrix} J_x & 0 & 0 \\ 0 & J_y & 0 \\ 0 & 0 & J_z \end{bmatrix} \quad (1)$$

be the diagonal inertia matrix of the spacecraft, $m=[M_x \ M_y \ M_z]^T$ be the control torques generated by the thrusters, and $h=[J_x w_x \ J_y w_y + h_w \ J_z w_z]^T$ be the inertial angular momentum vector of the spacecraft, then (see Wertz 1978)

$$\dot{h} = J\dot{W} = -W \times h + m = h \times W + m \quad (2)$$

or equivalently

$$\begin{bmatrix} J_x & 0 & 0 \\ 0 & J_y & 0 \\ 0 & 0 & J_z \end{bmatrix} \begin{bmatrix} \dot{w}_x \\ \dot{w}_y \\ \dot{w}_z \end{bmatrix} = \begin{bmatrix} 0 & -J_z w_z & J_y w_y + h_x \\ J_z w_z & 0 & -J_x w_x \\ -J_y w_y - h_w & J_x w_x & 0 \end{bmatrix} \begin{bmatrix} w_x \\ w_y \\ w_z \end{bmatrix} + \begin{bmatrix} M_x \\ M_y \\ M_z \end{bmatrix} \quad (3)$$

In view of Fig. 2, the matrices of thruster force directions \vec{F} and moment arms \vec{R} in the body frame are given as

$$\vec{F} = [f_1 \quad f_2 \quad f_3 \quad f_4] = \begin{bmatrix} -a & -a & a & a \\ a & -a & -a & a \\ 1 & 1 & 1 & 1 \end{bmatrix} \quad (4)$$

and

$$\vec{R} = [r_1 \quad r_2 \quad r_3 \quad r_4] = \begin{bmatrix} -d & -d & d & d \\ -d & d & d & -d \\ l & l & l & l \end{bmatrix} \quad (5)$$

where $a = \frac{\sqrt{2}}{2} \sin\left(5 \times \frac{\pi}{180}\right) \approx 0.707 \times 5 \times \frac{\pi}{180}$, columns 1, 2, 3, and 4 represent the thrusters 1, 2, 3, and 4. Denote $T_1, T_2, T_3,$ and T_4 the thruster levels of thrusters 1, 2, 3, and 4. Let

$$u = [T_1 \quad T_2 \quad T_3 \quad T_4]^T$$

be the level control vector, then the control torque m can be expressed as

$$m = \begin{bmatrix} r_1 \times f_1 & r_2 \times f_2 & r_3 \times f_3 & r_4 \times f_4 \end{bmatrix} \begin{bmatrix} T_1 \\ T_2 \\ T_3 \\ T_4 \end{bmatrix} \quad (6)$$

Adjoining Eq. (3) and Eq. (6) gives

$$\begin{bmatrix} \dot{w}_x \\ \dot{w}_y \\ \dot{w}_z \end{bmatrix} = \begin{bmatrix} 0 & -\frac{J_z w_z}{J_x} & \frac{J_y w_y + h_x}{J_x} \\ \frac{J_z w_z}{J_y} & 0 & -\frac{J_x w_x}{J_y} \\ -\frac{J_y w_y + h_w}{J_z} & \frac{J_x w_x}{J_z} & 0 \end{bmatrix} \begin{bmatrix} w_x \\ w_y \\ w_z \end{bmatrix} + \begin{bmatrix} \frac{1}{J_x} & 0 & 0 \\ 0 & \frac{1}{J_y} & 0 \\ 0 & 0 & \frac{1}{J_z} \end{bmatrix} \begin{bmatrix} r_1 \times f_1 \\ r_2 \times f_2 \\ r_3 \times f_3 \\ r_4 \times f_4 \end{bmatrix}^T \begin{bmatrix} T_1 \\ T_2 \\ T_3 \\ T_4 \end{bmatrix} \quad (7)$$

According to Yang (2010), for $\alpha \in (-\pi, \pi)$, the vector part of the quaternion q meets the following relation

$$\begin{bmatrix} \dot{q}_1 \\ \dot{q}_2 \\ \dot{q}_3 \end{bmatrix} = \frac{1}{2} \begin{bmatrix} \sqrt{1-q_1^2-q_2^2-q_3^2} & -q_3 & q_2 \\ q_3 & \sqrt{1-q_1^2-q_2^2-q_3^2} & -q_1 \\ -q_2 & q_1 & \sqrt{1-q_1^2-q_2^2-q_3^2} \end{bmatrix} \begin{bmatrix} w_x \\ w_y \\ w_z \end{bmatrix} \quad (8)$$

The linearized form of Eq. (7) is given as

$$\begin{bmatrix} \dot{w}_x \\ \dot{w}_y \\ \dot{w}_z \end{bmatrix} = \begin{bmatrix} 0 & 0 & \frac{h_w}{J_x} \\ 0 & 0 & 0 \\ -\frac{h_w}{J_z} & 0 & 0 \end{bmatrix} \begin{bmatrix} w_x \\ w_y \\ w_z \end{bmatrix} + \begin{bmatrix} J_x^{-1} & 0 & 0 \\ 0 & J_y^{-1} & 0 \\ 0 & 0 & J_z^{-1} \end{bmatrix} \begin{bmatrix} r_1 \times f_1 \\ r_2 \times f_2 \\ r_3 \times f_3 \\ r_4 \times f_4 \end{bmatrix}^T \begin{bmatrix} T_1 \\ T_2 \\ T_3 \\ T_4 \end{bmatrix} \quad (9)$$

The linearized form of Eq. (8) is given as

$$\begin{bmatrix} \dot{q}_1 \\ \dot{q}_2 \\ \dot{q}_3 \end{bmatrix} = \frac{1}{2} \begin{bmatrix} 1 & 0 & 0 \\ 0 & 1 & 0 \\ 0 & 0 & 1 \end{bmatrix} \begin{bmatrix} w_x \\ w_y \\ w_z \end{bmatrix} \quad (10)$$

Adjoining Eqs. (9) and (10) gives the linearized quaternion based thruster control system equation as follows

$$\begin{bmatrix} \dot{w}_x \\ \dot{w}_y \\ \dot{w}_z \\ \dot{q}_1 \\ \dot{q}_2 \\ \dot{q}_3 \end{bmatrix} = \begin{bmatrix} 0 & 0 & \frac{h_w}{J_x} & 0 & 0 & 0 \\ 0 & 0 & 0 & 0 & 0 & 0 \\ -\frac{h_w}{J_x} & 0 & 0 & 0 & 0 & 0 \\ .5 & 0 & 0 & 0 & 0 & 0 \\ 0 & .5 & 0 & 0 & 0 & 0 \\ 0 & 0 & .5 & 0 & 0 & 0 \end{bmatrix} \begin{bmatrix} w_x \\ w_y \\ w_z \\ q_1 \\ q_2 \\ q_3 \end{bmatrix} + \begin{bmatrix} J_x^{-1} & 0 & 0 \\ 0 & J_y^{-1} & 0 \\ 0 & 0 & J_z^{-1} \\ 0 & 0 & 0 \\ 0 & 0 & 0 \\ 0 & 0 & 0 \end{bmatrix} \begin{bmatrix} r_1 \times f_1 \\ r_2 \times f_2 \\ r_3 \times f_3 \\ r_4 \times f_4 \end{bmatrix}^T \begin{bmatrix} T_1 \\ T_2 \\ T_3 \\ T_4 \end{bmatrix} := Ax + bu \quad (11)$$

where

$$A = \begin{bmatrix} 0 & 0 & \frac{h_w}{J_x} & 0 & 0 & 0 \\ 0 & 0 & 0 & 0 & 0 & 0 \\ -\frac{h_w}{J_x} & 0 & 0 & 0 & 0 & 0 \\ .5 & 0 & 0 & 0 & 0 & 0 \\ 0 & .5 & 0 & 0 & 0 & 0 \\ 0 & 0 & .5 & 0 & 0 & 0 \end{bmatrix},$$

and

$$B = \begin{bmatrix} J_x^{-1} & 0 & 0 \\ 0 & J_y^{-1} & 0 \\ 0 & 0 & J_z^{-1} \\ 0 & 0 & 0 \\ 0 & 0 & 0 \\ 0 & 0 & 0 \end{bmatrix} \begin{bmatrix} r_1 \times f_1 & r_2 \times f_2 & r_3 \times f_3 & r_4 \times f_4 \end{bmatrix}.$$

For the convenience of the computer control system design, following the same steps performed in Stoltz *et al.* (1998), the continuous system is converted to a discrete form given by

$$x_6(n+1) = \Phi_6 x_6(n) + \Gamma_{6 \times 4} u(n) \quad (12)$$

where $x_6 = [w_x \ w_y \ w_z \ q_1 \ q_2 \ q_3]^T$, $\Phi_6 = e^{A \cdot dT}$, $\Gamma_{6 \times 4} = \int_0^{dT} e^{A(t-\tau)} B d\tau$, and $dT = 4(\text{sec})$ is the sample period (the same number is used in Stoltz *et al.* (1998)). It is shown in Stoltz *et al.* (1998) that using the integral terms of Euler angles in controller design is very successful for orbit-raising. To incorporate the integral terms of quaternion, the discrete integrators

$$iq = [iq_1 \ iq_2 \ iq_3]^T = \begin{bmatrix} \int_0^{dT} q_1 \\ \int_0^{dT} q_2 \\ \int_0^{dT} q_3 \end{bmatrix}^T$$

are simply as

$$iq(n+1) = iq(n) + dT * q(n) \quad (13)$$

where $q(n)$ is the vector value of the reduced quaternion at the n th sample period. Adjoining Eqs. (12) and (13) gives

$$x_9(n+1) = \begin{bmatrix} x_6(n+1) \\ iq(n+1) \end{bmatrix} = \begin{bmatrix} \Phi_6 & 0_{6 \times 3} \\ dT[0_{3 \times 3} & I_{3 \times 3}] & I_{3 \times 3} \end{bmatrix} \begin{bmatrix} x_6(n) \\ iq(n) \end{bmatrix} + \begin{bmatrix} \Gamma_{6 \times 4} \\ 0_{3 \times 4} \end{bmatrix} u(n) \quad (14)$$

3. LQR design and pulse width modulation

For orbit-raising using Hohmann transfers, the thrust control requires that the four thrusters must fire in a controlled manner so that the spacecraft will accelerate in the z direction depicted as in Fig. 3. This means that the quaternion and the angular rate relative to the frame depicted as in the Fig. 3 should be as small as possible. Therefore, the thrust control design is to select control $u(n)$ to maintain the attitude in the orbit-raising operation. This can be represented as a LQR design which minimizes the cost function

$$J = \frac{1}{2} \sum_0^\infty [x^T(n)Qx(n) + u^T(n)Ru(n)]$$

under the constraint of (14). The discrete state feedback control can be obtained using the MATLAB control toolbox (Grace *et al.* 1990).

$$u(n) = -Kx_9(n) \quad (15)$$

where K is a 4×9 state feedback matrix. It is worthwhile to note (a) this design considers only the attitude control problem but does not really consider the thrust level selection, and (b) the designed control force may take negative value but OrbView-2 thrusters thrust only in positive direction. Stoltz *et al.* (1998) provided a nice method to convert the LQR controller to a pulse width modulation. Notice that OrbView-2 thrusters are operated using an on/off switch to control the pulse width, thereby to control the thrust force (level). The suggested procedure to convert the LQR controller to pulse width modulation is as follows (Stoltz *et al.* 1998):

1. Compute the LQR thruster commands: $u(n) = -Kx_9(n)$
2. Convert from variable thrusts $u(n)$ for the fixed total sample period dT to fixed thrusts f for variable times $t_i(n)$: Use the identity $u_i(n) * dT = f * t_i(n)$ and design parameter $f = 1(lbf) = 4.448(N)$ as the thrust force magnitude, then, the i th thruster on-time $t_i(n) = \frac{dT * u_i(n)}{f}$, for $i=1, 2, 3, 4$.
3. Limit on-times to \pm half the sample period, i.e., $0.5dT \leq t_i(n) \leq 0.5dT$.
4. Compute a bias term t_b such that $\max_i\{t_i(n) + t_b\} = dT$, add the bias to all on-times such that at least one thruster is on for the complete sample period.

Remark 3.1 It is easy to see that the bias term is the thrust term, while $t_i(n)$ terms are used to control the attitude during the thrust period.

Similar to Stoltz *et al.* (1998), it is assumed that thruster valve actuators significantly disturb the measurement of magnetometer, so the magnetometer is read only in the two second period when the thrusters are off. To maintain the same force $u(n)$ in every 4 seconds of a sample period, the thruster commands, $u(n)$, are doubled and the thruster on-times halved to a maximum of two seconds out of every four second sample period.

4. Comparison of quaternion based and Euler angle based designs

In this section, two different orbit-raising designs, the design based on the reduced quaternion model established in Section 2 and the design based on the Euler angle model given in Stoltz *et al.* (1998), are compared. Both designs use standard LQR design method with the same spacecraft parameters as provided in Stoltz *et al.* (1998). In particular, the sample period is 4 seconds; the maximum thruster on-time is 2 seconds; the diagonal elements of the inertia matrix are $J_x=189$ ($\text{kg}\cdot\text{m}^2$), $J_y=159$ ($\text{kg}\cdot\text{m}^2$), $J_z=114$ ($\text{kg}\cdot\text{m}^2$); the momentum wheel moment is -2.8 ($\text{N}\cdot\text{m}\cdot\text{sec}$); the diagonal elements of the Q matrix are $Q_1=Q_2=Q_3=1/(2.5\text{rad/sec})^2$ and $Q_4=Q_5=Q_6=1/(9\text{rad})^2$, $Q_7=Q_8=Q_9=1/(182\text{rad}\cdot\text{sec})^2$; the diagonal elements of the R matrix are $R_1=R_2=R_3=R_4=1\text{N}^2$. It is assumed further that the same thrusters are installed and the same alignments are used as in Fig. 2 where $d=0.248$ m and $l=0.8151$ m. The LQR design based on the Euler angle model has been successfully used for the OrbView-2 orbit-raising and the results have been reported in (Stoltz *et al.* 1998). Using the parameters listed above for the design model described in Stoltz *et al.* (1998) and applying dlqr command in MATLAB toolbox (Grace *et al.* 1990) yield the feedback matrix

$$K_e = \begin{bmatrix} -13.4793 & 7.2831 & -23.0823 & 0.1696 & 0.2041 & -0.4353 & 0.0008 & 0.0026 & -0.0036 \\ 13.4793 & 7.2831 & 23.0823 & -0.1696 & 0.2041 & 0.4353 & -0.0008 & 0.0026 & 0.0036 \\ 10.3283 & -7.2831 & -11.4276 & 0.4938 & -0.2041 & 0.0255 & 0.0037 & -0.0026 & 0.0007 \\ -10.3283 & -7.2831 & 11.4276 & -0.4938 & -0.2041 & -0.0255 & -0.0037 & -0.0026 & -0.0007 \end{bmatrix}$$

For the reduced quaternion model (14) with the same set of parameters listed above, applying dlqr command in MATLAB toolbox yields the feedback matrix of the LQR design

$$K_q = \begin{bmatrix} -10.3382 & 5.7669 & -15.8921 & 0.3123 & 0.2545 & -0.5028 & 0.0013 & 0.0026 & -0.0035 \\ 10.3382 & 5.7669 & 15.8921 & -0.3123 & 0.2545 & 0.5028 & -0.0013 & 0.0026 & 0.0035 \\ 8.1974 & -5.7669 & -7.9309 & 0.6542 & -0.2545 & 0.0959 & 0.0036 & -0.0026 & 0.0012 \\ -8.1974 & -5.7669 & 7.9309 & -0.6542 & -0.2545 & -0.0959 & -0.0036 & -0.0026 & -0.0012 \end{bmatrix}$$

These feedback matrices (K_e and K_q) are applied to the original nonlinear system. For both Euler angle model and quaternion model, Eq. (7) is used to represent the nonlinear dynamics of motion which has its discretized form as follows

$$\begin{bmatrix} w_x(n+1) \\ w_y(n+1) \\ w_z(n+1) \end{bmatrix} = \begin{bmatrix} 1 & -dT \frac{J_z w_z(n)}{J_x} & dT \frac{J_y w_y(n) + h_w}{J_x} \\ dT \frac{J_z w_z(n)}{J_y} & 1 & -dT \frac{J_x w_x(n)}{J_y} \\ dT \frac{J_y w_y(n) + h_w}{J_z} & dT \frac{J_x w_x(n)}{J_z} & 1 \end{bmatrix} \begin{bmatrix} w_x(n) \\ w_y(n) \\ w_z(n) \end{bmatrix} - dT \begin{bmatrix} J_x^{-1} & 0 & 0 \\ 0 & J_y^{-1} & 0 \\ 0 & 0 & J_z^{-1} \end{bmatrix} \begin{bmatrix} r_1 \times f_1 \\ r_2 \times f_2 \\ r_3 \times f_3 \\ r_4 \times f_4 \end{bmatrix}^T Kx_9(n) \quad (16)$$

where K is either K_e or K_q . For Euler angle model, the nonlinear kinematics equation of motion is given as Kuipers (1999)

$$\begin{bmatrix} \dot{\phi} \\ \dot{\theta} \\ \dot{\psi} \end{bmatrix} = \begin{bmatrix} 1 & \sin(\phi) \tan(\theta) & \cos(\phi) \tan(\theta) \\ 0 & \cos(\phi) & -\sin(\phi) \\ 0 & \sin(\phi) \sec(\theta) & \cos(\phi) \sec(\theta) \end{bmatrix} \begin{bmatrix} w_x \\ w_y \\ w_z \end{bmatrix} \quad (17)$$

which has its discretized form as follows

$$\begin{bmatrix} \phi(n+1) \\ \theta(n+1) \\ \psi(n+1) \end{bmatrix} = dT \begin{bmatrix} 1 & \sin(\phi(n)) \tan(\theta(n)) & \cos(\phi(n)) \tan(\theta(n)) \\ 0 & \cos(\phi(n)) & -\sin(\phi(n)) \\ 0 & \sin(\phi(n)) \sec(\theta(n)) & \cos(\phi(n)) \sec(\theta(n)) \end{bmatrix} \begin{bmatrix} w_x(n) \\ w_y(n) \\ w_z(n) \end{bmatrix} + \begin{bmatrix} \phi(n) \\ \theta(n) \\ \psi(n) \end{bmatrix} \quad (18)$$

For reduced quaternion model, the nonlinear kinematics equation of motion is given by Eq. (8) which has its discretized form as follows

$$\begin{bmatrix} q_1(n+1) \\ q_2(n+1) \\ q_3(n+1) \end{bmatrix} = \frac{dT}{2} \begin{bmatrix} \sqrt{1-q_1^2(n)-q_2^2(n)-q_3^2(n)} w_x(n) - q_3(n) w_y(n) + q_2(n) w_z(n) \\ q_3(n) w_x(n) + \sqrt{1-q_1^2(n)-q_2^2(n)-q_3^2(n)} w_y(n) - q_1(n) w_z(n) \\ -q_2(n) w_x(n) + q_1(n) w_y(n) + \sqrt{1-q_1^2(n)-q_2^2(n)-q_3^2(n)} w_z(n) \end{bmatrix} + \begin{bmatrix} q_1(n) \\ q_2(n) \\ q_3(n) \end{bmatrix} \quad (19)$$

Eq. (13) is used to propagate the 3 quaternion integral states for the quaternion feedback control. For the Euler angle feedback control, the discrete Euler angle integrators

$$ie = [ie_1 \quad ie_2 \quad ie_3]^T = \begin{bmatrix} \int_0^{dT} \phi \\ \int_0^{dT} \theta \\ \int_0^{dT} \psi \end{bmatrix}^T$$

is given by

$$ie(n+1) = ie(n) + dT * d(n) \quad (20)$$

to propagate the last 3 integral states where $d(n)=[\phi(n), \theta(n), \psi(n)]^T$.

Since other disturbance torques (Wertz 1978), such as gravity gradient torque, aerodynamic drag, geopotential induced torque, and solar pressure torque are very small comparing to the thrust torques, these disturbance torques are ignored in our simulation.

In the simulation tests, the following initial conditions are assumed: the initial quaternion rates are zeros; the initial Euler angles are 2 degrees in roll, pitch, and yaw; the initial Euler angles are converted to initial quaternion and used as the initial feedback in quaternion model based design; the initial integral terms for reduced quaternion model and for Euler angles model are all set to zeros. At the end of every iteration in quaternion based design simulation, the quaternion is converted back to the Euler angles and saved so that the responses of the two different designs can be compared using the same error measurement.

The simulation results are provided in Figs. 4-13. In these figures, the solid lines are the responses and/or controls of the quaternion based design; the dashed lines are the responses and/or controls of the Euler angle based design. Both designs have similar responses in terms of widely used indices such as percentage of overshoot, settling time, etc (Dorf and Bishop 2008). The total (summation) thrust time used for attitude control in the quaternion based design (12.0006 seconds)

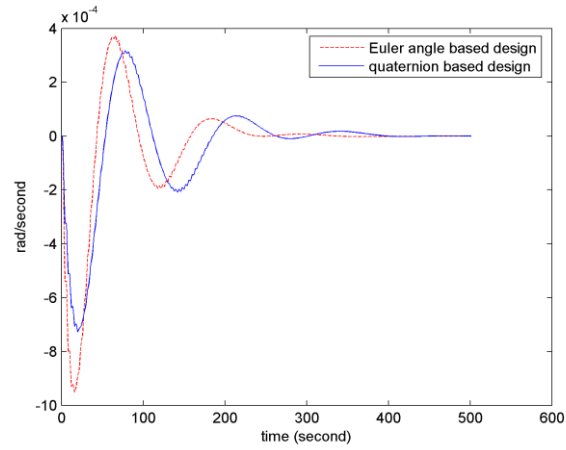


Fig. 4 Design comparison for quaternion rate w_1

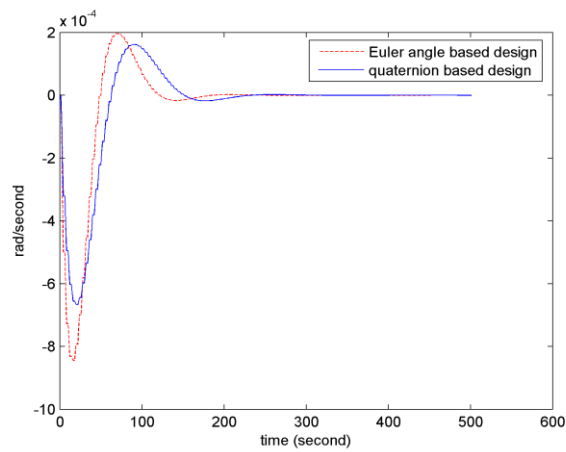


Fig. 5 Design comparison for quaternion rate w_2

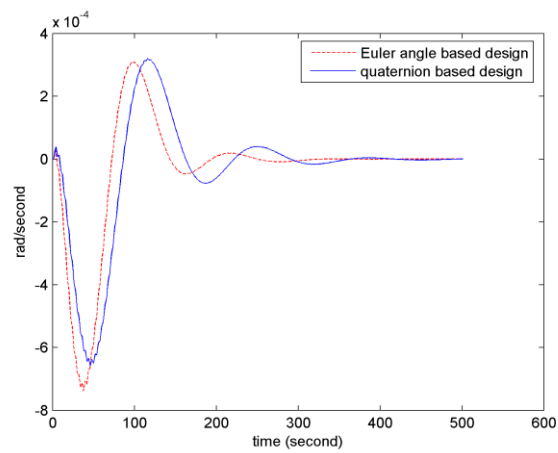


Fig. 6 Design comparison for quaternion rate w_3

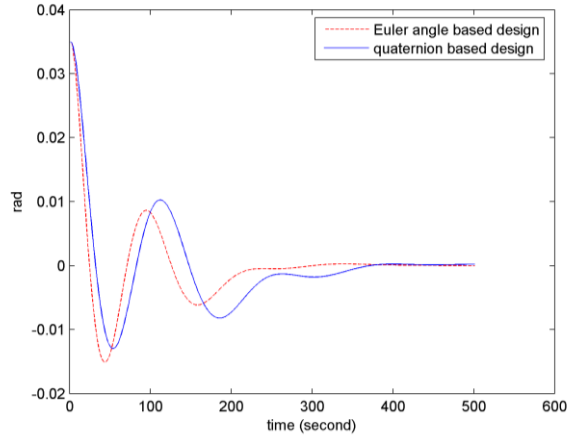


Fig. 7 Design comparison for quaternion q_1

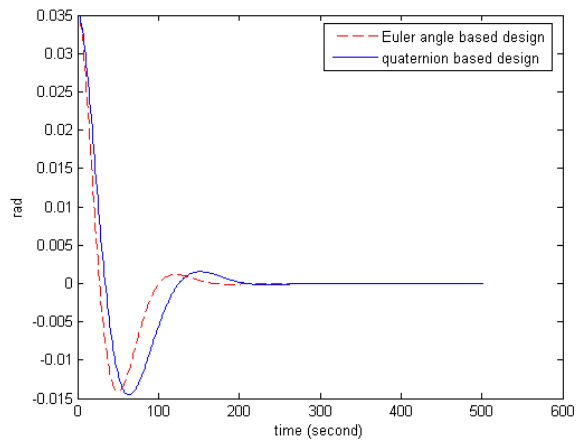


Fig. 8 Design comparison for quaternion q_2

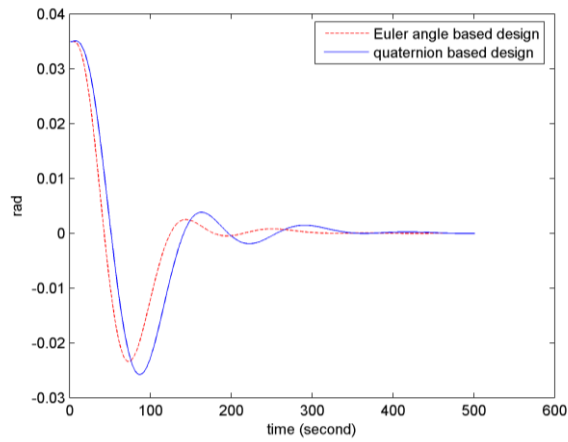


Fig. 9 Design comparison for quaternion q_3

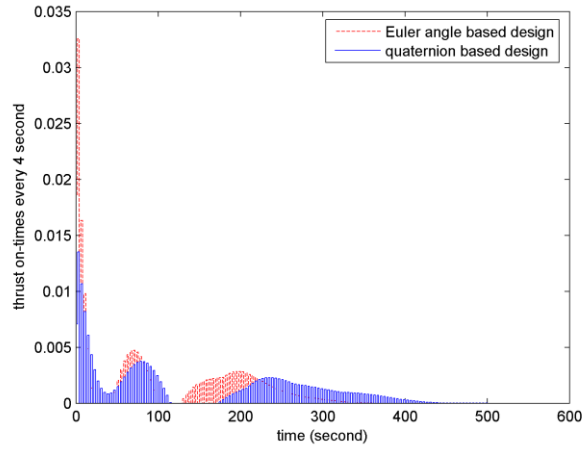


Fig. 10 Design comparison for Thrust u_1

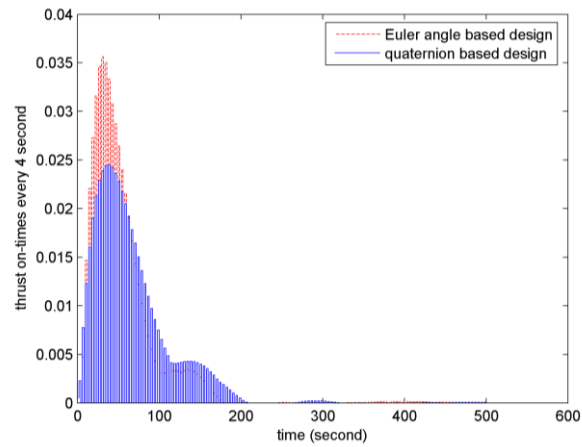


Fig. 11 Design comparison for Thrust u_2

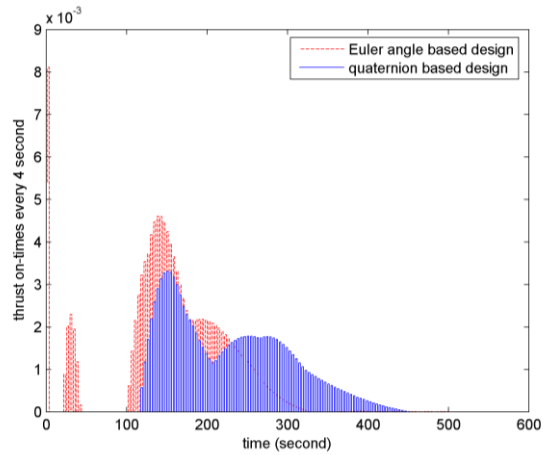


Fig. 12 Design comparison for Thrust u_3

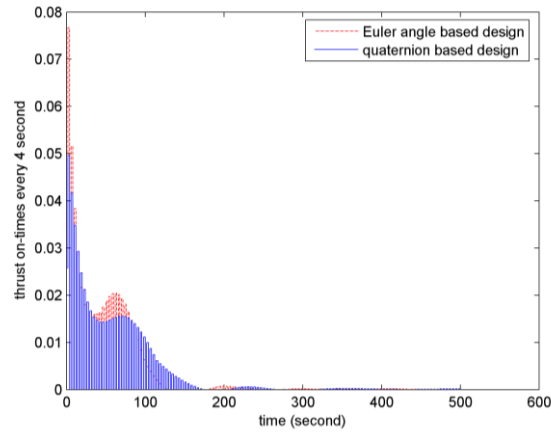


Fig. 13 Design comparison for Thrust u_4

is slightly better than the total (summation) thrust time used for attitude control in the Euler angle based design (12.6352 seconds) during 500 second thrust period, which means that the fuel consumption using the quaternion based design is less than the Euler angle based design. But the most important advantages in quaternion based design comparing to the Euler angle based design, as pointed before, are (a) the model is independent to the rotational sequence; (b) the singular point is the farthest to the point where the linearization is carried out; and (c) the quaternion measurement is readily available onboard for most satellites.

5. Conclusions

In this paper, a reduced quaternion model for spacecraft attitude control systems in orbit-raising mode is derived. Simulations for two LQR designs based on two different models, the reduced quaternion model and the Euler angle model, are conducted. These simulations show that the control system design based on the reduced quaternion model is a promising technique.

Acknowledgments

The author would like to thank Mr. Mike Case, the Director of the Division of Engineering in the Office of Research at US NRC, and Dr. Chris Hoxie, in the Office of Research at US NRC for their providing computational environment for this research.

References

- Athans, M. and Falb, P.L. (1966), *Optimal Control: An Introduction to the Theory and Its Applications*, McGraw-Hill Inc., New York, USA.
- Boskovic, J., Li, S. and Mehra, R. (2001), "Robust adaptive variable structure control of spacecraft under control input saturation", *J. Guid. Control Dyn.*, **24**(1), 14-22.

- Bras, S., Rosa, P., Silvestre, C. and Oliverira, P. (2013), "Global attitude and gyro-bias estimation based on set-valued observers", *Syst. Control Lett.*, **62**(7), 937-942.
- Chan, B., Park, Y., Roh, W. and Cho, G. (2010), "Attitude controller design and test of Korea Space Launch Vehicle-I", *Int. J. Aeronaut. Space Sci.*, **11**(2), 303-314.
- Chen, C., Shun, Y., Cheng, C., Liao, P. and Fang, Z. (2007), "MATLAB-based rapid controller development platform for control applications", *Proc. IMechE Part C: J. Mech. Eng. Sci.*, **221**(11), 1461-1473.
- Dorf, R.C. and Bishop, R.H. (2008), *Modern Control Systems*, Pearson Prentice Hall, Upper Saddle River, NJ, USA.
- Grace, A., Laub, A.J., Little, J.N. and Thompson, C. (1990), *Control system toolbox for use with MATLAB*, User's Guide, The MathWorks Inc., South Natick, MA, USA.
- Kim, D., Park, S., Kim, J. and Choi, K. (2008), "Development of a hardware in the loop simulation for spacecraft attitude control using a momentum wheel", *J. Astronaut. Space Sci.*, **25**(2), 347-360.
- Kuipers, J.B. (1999), *Quaternions and Rotation Sequences: A Primer with Applications to Orbits, Aerospace and Virtual Reality*, Princeton University Press, Princeton, New Jersey, USA.
- Martin, P. and Salaun, E. (2010), "Design and implementation of a low-cost observer-based attitude and heading reference system", *Control Eng. Prac.*, **18**(7), 712-722.
- Noll, R.B., Zvara, J. and Deyst, J.J. (1971), *Spacecraft Attitude Control During Thrusting Maneuvers: Spacecraft Spin Stabilized Thrust Control*, NASA space vehicle design criteria, NASA SP-8059.
- Paielli, R. and Bach, R. (1993), "Control with realization of linear error dynamics", *J. Guid. Control Dyn.*, **16**(1), 182-189.
- Sanyal, A., Lee, T., Leok, M. and McClamroch, N. (2008), "Global optimal attitude estimation using uncertainty ellipsoids", *Syst. Control Lett.*, **57**(3), 236-254.
- Show, L.L., Juang, J.C. and Jan, Y.W. (2003), "An LMI-based nonlinear attitude approach", *IEEE Tran. Control Syst. Tech.*, **11**(1), 73-83.
- Sidi, M. (1997), *Spacecraft Dynamics and Control: A Practical Engineering Approach*, Cambridge University Press, Cambridge, UK.
- Stoltz, P.M., Sivapiragasam, S. and Anthony, T. (1998), "Satellite orbit-raising using LQR control with fixed thrusters", *Proceedings of the 21st Annual AAS Rocky Mountain Guidance and Control Conference*, Brackenridge, CO, USA, February.
- Wallsgrove, R. and Akella, M. (2005), "Globally stabilizing saturated control in the presence of bounded unknown disturbances", *J. Guid. Control Dyn.*, **28**(5), 957-963.
- Wen, J. and Kreutz-Delgado, K. (1991), "The attitude control problem", *IEEE Tran. Automat. Control*, **36**(10), 1148-1161.
- Wertz, J. (1978), *Spacecraft Attitude Determination and Control*, Kluwer Academic Publishers, Dordrecht, Holland.
- Wie, B. (1998), *Vehicle Dynamics and Control*, AIAA Education Series, Reston, VA, USA.
- Wie, B., Weiss, H. and Arapostathis, A. (1989), "Quaternion feedback regulator for spacecraft eigenaxis rotations", *J. Guid. Control Dyn.*, **12**(2), 375-380.
- Won, C. (1999), "Comparative study of various control methods for attitude control of a LEO satellite", *Aerosp. Sci. Tech.*, **3**(5), 323-333.
- Yang, Y. (2010), "Quaternion based model for momentum biased nadir pointing spacecraft", *Aerosp. Sci. Tech.*, **14**(3), 199-202.
- Yang, Y. (2012), "Analytic LQR design for spacecraft control system based on quaternion model", *J. Aerosp. Eng.*, **25**(3), 448-453.
- Yang, Y. (2012a), "Spacecraft attitude determination and control: Quaternion based method", *Ann. Rev. Control*, **36**(2), 198-219.
- Yang, Y. (2014), "Quaternion based LQR spacecraft control design is a robust pole assignment design", *J. Aerosp. Eng.*, **27**(1), 168-176.